Temperature Dependence of the Optical Transition Energies of Carbon Nanotubes: The Role of Electron-Phonon Coupling and Thermal Expansion

S. B. Cronin,[1,2,*] Y. Yin,[3] A. Walsh,[3] Rodrigo B. Capaz,[4,6] A. Stolyarov,[2] P. Tangney,[5] Marvin L. Cohen,[6] Steven G. Louie,[5,6] A. K. Swan,[3] M. S. Ünlü,[3,7] B. B. Goldberg,[3,7] and M. Tinkham[2]

[1]*Department of Electrical Engineering, University of Southern California, Los Angeles, California 90098, USA*
[2]*Department of Physics, Harvard University, Cambridge, Massachusetts 02138, USA*
[3]*Department of Physics, Boston University, Boston, Massachusetts 02215, USA*
[4]*Universidade Federal do Rio de Janeiro, Caixa Postal 68528, Rio de Janeiro, RJ 21941-972, Brazil*
[5]*The Molecular Foundry, Lawrence Berkeley National Laboratory, Berkeley, California 94720, USA*
[6]*Department of Physics, University of California at Berkeley, and Materials Sciences Division, Lawrence Berkeley National Laboratory, Berkeley, California 94720, USA*
[7]*Department of Electrical and Computer Engineering, Boston University, Boston, Massachusetts 02215, USA*

(Received 2 August 2005; published 30 March 2006)

Tunable Raman spectroscopy is used to measure the optical transition energies E_{ii} of individual single wall carbon nanotubes. E_{ii} is observed to shift down in energy by as much as 50 meV, from -160 to 300 °C, in contrast with previous measurements performed on nanotubes in alternate environments, which show upshifts and downshifts in E_{ii} with temperature. We determine that electron-phonon coupling explains our experimental observations of nanotubes suspended in air, neglecting thermal expansion. In contrast, for nanotubes in surfactant or in bundles, thermal expansion of the nanotubes' environment exerts a nonisotropic pressure on the nanotube that dominates over the effect of electron-phonon coupling.

DOI: 10.1103/PhysRevLett.96.127403 PACS numbers: 78.67.Ch, 73.22.−f, 78.30.Na

The temperature dependence of the electronic band structure of carbon nanotubes is important for many of their practical applications such as field-effect transistors [1] and single nanotube optical emission devices [2]. With a precise understanding of the temperature dependence of nanotubes we are able to use the temperature as a parameter to *tune* the electronic energies of nanotubes in a controlled manner, thus providing a more versatile set of devices, as well as a better understanding of the fundamental physics of carbon nanotubes.

In earlier work, Raman spectroscopy carried out at a fixed laser energy on large ensembles of nanotubes showed downshifts in the phonon frequencies with increasing temperature [3,4]. The results also indicated that the optical transition energies E_{ii} [5] shift with temperature, although they were unable to determine by how much E_{ii} shifted or in which direction. More recently, photoluminescence spectroscopy and tunable Raman spectroscopy have allowed the direct measurement of the optical transition energies E_{ii} as a function of temperature [7–14]. These studies show a variety of results ranging in both the magnitude and sign of the shift dE_{ii}/dT. Studies on nanotube bundles [13] and nanotubes coated in surfactant [9,13,14] show dE_{ii}/dT to be positive or negative, depending on whether $(n - m)\text{mod}3 = 1$ or 2, respectively.

In the present work, E_{ii} of individual isolated nanotubes suspended over trenches are measured at various temperatures using tunable Raman spectroscopy. By suspending the nanotubes off the substrate we minimize the environmental perturbation to the nanotube, and are thus able to observe the theoretically predicted electron-phonon coupling behavior in nanotubes [15]. This behavior is not observed in nanotubes in alternate environments, where the thermal effect is dominated by pressures exerted due to the expansion and contraction of the nanotubes' environment.

Individual suspended single wall carbon nanotubes (SWNTs) are prepared by first etching trenches in quartz substrates by reactive ion etching (RIE) in a CF_4 plasma. A chromium film, patterned by electron beam lithography and wet chemical etching, is used to mask the quartz during the RIE process. SWNTs are grown over the trenches by chemical vapor deposition in methane gas at 900 °C, using a 1 nm thick film of iron as the catalyst for the nanotube growth. Resonant nanotubes are found by scanning the laser spot along the trench. We typically find 3 to 5 spatially separated resonant nanotubes along the 77 μm long trench. Once a resonant nanotube is found with an extremely large signal, we record its location. While atomic force microscopy and scanning electron microscopy (SEM) were performed on preliminary samples to optimize the parameters of our growth of individual suspended nanotubes, microscopy was not performed on the samples measured in this work. We found that SEM exposure spoiled the strong resonance we observed in pristine samples. Spectra are measured in a modified Renishaw Raman microprobe RM1000B, with a tunable Ti:sapphire laser and variable angle filters allowing us to tune through the resonance of an individual nanotube between 720 and 830 nm (1.72 to 1.49 eV). For the diameter distribution of these samples we are primarily in resonance with E_{11} of metallic nanotubes and E_{22} of semiconducting nanotubes. Spectra were taken with a 50× objective (NA = 0.75) at a laser power of 1 mW. The sample temperature was con-

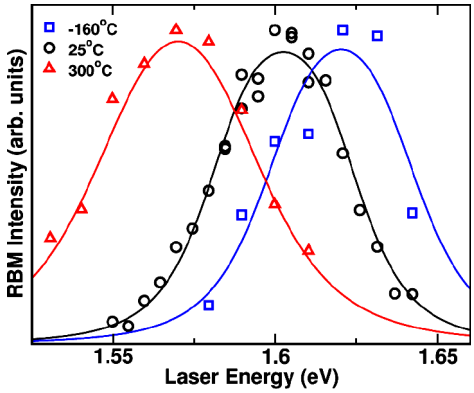

FIG. 1 (color online). Radial breathing mode intensity of an individual suspended SWNT plotted as a function of laser energy for three different temperatures. The solid lines show theoretical fits to the experimental data. The peak intensities at each temperature are normalized for better graphical representation.

trolled with a Linkam (THMS600) temperature control system over the range −160 to 300 °C in a N_2 gas environment. Additional heating from the laser is ruled out by the Stokes/anti-Stokes ratio which produces the expected value at room temperature, based on the Maxwell-Boltzmann factor $e^{-E_{\rm ph}/k_BT}$ [16].

Figure 1 shows the intensity of the 268 $\rm cm^{-1}$ radial breathing mode (RBM) of an individual suspended SWNT plotted as a function of laser energy at three different temperatures. Each point on this plot corresponds to the RBM intensity taken at a different laser energy. At each temperature the intensity profile depicts a well-defined peak indicating the resonance condition between the laser energy and the transition energy E_{ii} of the SWNT. We notice that the position of the peak intensity shifts down in energy by about 50 meV over this temperature range. The RBM intensities at these three temperatures are normalized for graphical purposes. We observe the intensity to decrease monotonically as the temperature increases, while the width of the resonance increases with temperature. The RBM frequency, however, is not observed to change with temperature, within the precision of the measurement.

The experimental data was fit using the resonant Raman scattering equation for a one dimensional (1D) system [12,16], yielding accurate values for the transition energies E_{ii} and the resonance broadening factor η. In this way we can determine E_{ii} directly from the measurement with ∼1.5 meV precision. Table I shows the results of least squares fitting of the experimental data to the resonant Raman equation. Since these nanotubes are suspended in air, and have been shown to be shifted in E_{ii} from those coated in surfactant [16], unambiguous (n, m) assignments of these nanotubes are not possible. The first two nanotubes in Table I with $\omega_{\rm RBM} = 267$ and 268 $\rm cm^{-1}$ are semiconducting, in resonance with E_{22}, and have been assigned to the $2n + m = 22$ branch [16]. It is likely that these are $(10, 2)$ and $(11, 0)$ nanotubes. The remaining three nanotubes fall in the range of metallic nanotubes [17], and are more difficult to assign (n, m). These metallic nanotubes are in either the branch $2n + m = 36$ or 39, with possible chiralities of $(18, 0)$, $(19, 1)$, $(12, 12)$, and $(14, 8)$.

TABLE I. Results of fitting of the tunable Raman data to the resonance Raman equation for five different individual suspended nanotubes. ΔE_{ii} (low T) and ΔE_{ii} (high T) correspond to $E_{ii}(300\ \rm K) - E_{ii}(113\ \rm K)$ and $E_{ii}(573\ \rm K) - E_{ii}(300\ \rm K)$, respectively, and are given in units of meV. The resonance broadening factor η and $d\eta/dT$ are given in units of meV and μeV/K, respectively.

Room Temperature			Temperature Dependence		
$\omega_{\rm RBM}$ ($\rm cm^{-1}$)	E_{ii} (eV)	η (meV)	ΔE_{ii} (low T)	ΔE_{ii} (high T)	$d\eta/dT$
268	1.586	17	−17.8	−32.4	13
267	1.579	14	−9.6	−11.3	9
179	1.575	19	−11.3	−19.4	50
160	1.574	20	−5.9	···	3
160	1.550	37	−1.0	−6.7	52

The optical transition energies in nanotubes are known to deviate from the single particle energies due to band gap renormalization and exciton binding [6,18,19]. As indicated by the equation $E(T, \epsilon) = E_{\rm SP}(T) + E_{\rm BGR}(\epsilon) - E_{\rm XB}(\epsilon)$, we expect the temperature dependence of the optical transition energy $E(T)$ to be determined primarily by the temperature dependence of the single particle energy $E_{\rm SP}(T)$, while the band gap renormalization energy $E_{\rm BGR}$ and exciton binding energy $E_{\rm XB}$ depend primarily on the dielectric constant ϵ rather than temperature [16].

The observed downshifts in E_{ii} can be explained by considering electron-phonon (e-p) coupling, calculated using a "frozen-phonon" scheme within an extended tight-binding model [15]. In this scheme, as the shape-deformation mode phonons become thermally occupied E_{ii} shifts down in energy over the temperature range of our measurements (−160 to 300 °C). Figure 2 and Table II show the temperature dependence of E_{ii} of some nanotubes whose diameters and transition energies correspond to those of the nanotubes measured in this experiment. For all of the nanotubes calculated, regardless of chirality, E_{ii} shifts down over the measured temperature range (−160 to 300 °C), as observed experimentally. For the $(11, 0)$ semiconducting nanotube, E_{22} shifts by −10.4 meV between −160 and 25 °C and by −19.8 meV between 25 and 300 °C. These theoretical predictions agree very well with the average experimental values in Table I. In Table I, the rate of change dE_{ii}/dT increases in magnitude with temperature, also in agreement with the e-p coupling model.

The temperature induced downshifts of E_{ii} (ΔE_{ii}) predicted by the e-p coupling model show relatively little dependence on chiral angle. For semiconducting nanotubes with $\nu = (n - m)\rm mod3 = 1$, ΔE_{22} tends to be smaller than for $\nu = 2$ nanotubes, particularly at low temperatures.

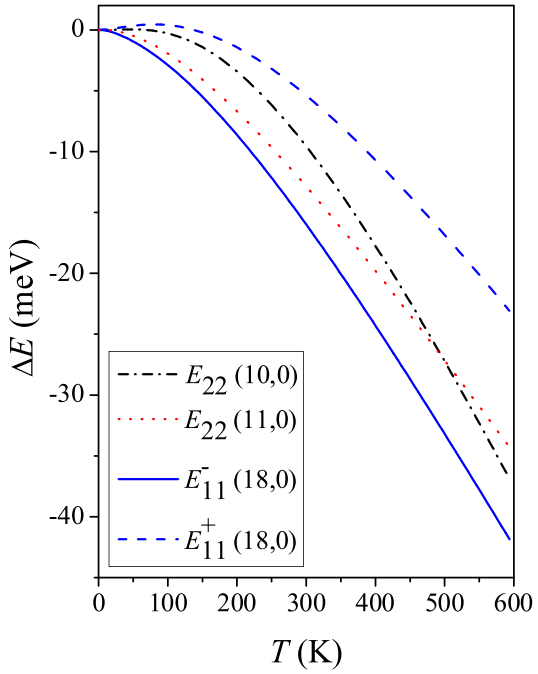

FIG. 2 (color online). Calculated shifts in the transition energies E_{ii} due to electron-phonon coupling for metallic (E_{11}) and semiconducting (E_{22}) nanotubes.

Also, the $\nu = 1$ nanotubes have a stronger dependence on nanotube diameter than the $\nu = 2$ nanotubes [15]. In metallic nanotubes, the first subband transition splits into an upper (E_{11}^{+}) and lower (E_{11}^{-}) band due to trigonal warping. E_{11}^{+} shows a weaker temperature dependence and a stronger diameter dependence than E_{11}^{-}. For both semiconducting and metallic nanotubes, larger diameter nanotubes tend to have smaller shifts in E_{ii}. The small ΔE_{ii} observed in the large diameter nanotubes of Table I ($\omega_{\mathrm{RBM}} = 160\ \mathrm{cm}^{-1}$) is consistent with this aspect of the e-p coupling model.

The consistent downshift of E_{ii} with increasing temperature, observed on nanotubes suspended in air, is in striking contrast to the tunable Raman and photoluminescence measurements on nanotubes in bundles [13] and surfactant coated nanotubes [9,13,14]. In both previous measurements E_{ii} is found to blueshift with increasing temperature for nanotubes with $\nu = 1$ and redshift for nanotubes with $\nu = 2$. A quantitative comparison of our work and the work on bundles is not possible since the laser heating method used does not yield the sample temperature. However, the qualitative disagreement between our measurements and these previous measurements is striking. The observed upshifts of E_{ii} cannot be explained by the e-p coupling model discussed above, and we must consider the effects of thermal expansion.

TABLE II. Calculated shifts in E_{ii} due to e-p coupling for metallic (E_{11}) and semiconducting (E_{22}) nanotubes. ΔE_{ii} (low T) and ΔE_{ii} (high T) correspond to $E_{ii}(300\ \mathrm{K}) - E_{ii}(113\ \mathrm{K})$ and $E_{ii}(573\ \mathrm{K}) - E_{ii}(300\ \mathrm{K})$, respectively, and are given in units of meV.

(n, m)	E_{ii}	ΔE_{ii} (low T)	ΔE_{ii} (high T)
(10, 0)	E_{22}	−9.1	−25.1
(10, 2)	E_{22}	−10.5	−20.5
(11, 0)	E_{22}	−10.4	−19.8
(13, 0)	E_{22}	−5.7	−16.6
(18, 0)	E_{11}^{-}	−12.4	−24.0
(18, 0)	E_{11}^{+}	−5.7	−16.3

We calculate the effect of expansion on the electronic subband energies using a simple nearest neighbor tight-binding model similar to that developed by Yang *et al.* [20,21]. All scenarios of expansion and nanotube diameter and chirality can be understood with a single analytical expression [22,23]:

$$\Delta E_{ii} = -2E_{ii}\epsilon_r - 3\gamma_0(-1)^i(-1)^\nu(\epsilon_r - \epsilon_z)\cos(3\theta), \tag{1}$$

where ϵ_r and ϵ_z are the radial and axial strains, θ is the chiral angle, and $\nu = (n - m)\mathrm{mod}3$ for semiconducting nanotubes and $\nu = 1$ for E_{11}^{-} and $\nu = 2$ for E_{11}^{+} transitions in metallic nanotubes. We can see from this expression that the effects of nonisotropic expansion on E_{ii} are maximized for zigzag nanotubes [$\cos(3\theta) = 1$]. For radial expansion ($\epsilon_z = 0$), E_{22} shifts down for $\nu = 1$ nanotubes and up for $\nu = 2$ nanotubes, as observed in the surfactant coated nanotubes. Conversely, for axial expansion ($\epsilon_r = 0$), E_{22} shifts up for $\nu = 1$ nanotubes and down for $\nu = 2$ nanotubes. For isotropic expansion ($\epsilon_r = \epsilon_z$) this expression reduces to $\Delta E_{ii} = -2E_{ii}\epsilon_r$, independent of chiral angle.

While radial expansion explains the experimental data from nanotubes in bundles [13] and nanotubes in surfactant [9], the effects of e-p coupling are expected to be present in all nanotubes regardless of their environment. However, pressure exerted by the thermal expansion of the nanotubes' environment dominates over the effect of e-p coupling. For surfactant coated nanotubes, the volume of the surfactant can be many times larger than that of the nanotube [24]. Assuming that the surfactant has a different thermal expansion coefficient than the nanotube it will exert a nonisotropic pressure on the nanotube because of the nanotube's very large aspect ratio. This conclusion has been put forth in a previous publication [10]. Therefore, the main effect of temperature for surfactant coated nanotubes is most likely the pressure exerted by the surfactant due to the thermal expansion or contraction of the surfactant, rather than the intrinsic thermal expansion of the nanotubes itself, which is negligible. A similar argument can be made for a nanotube in a bundle.

Further evidence exists for the influence of the thermal expansion of nanotubes' environment on E_{ii}. Li *et al.* studied the effects of strain induced in surfactant coated nanotubes by the thermal expansion/compression in D_2O using photoluminescence spectroscopy [10,11]. They observe both upshifts and downshifts in E_{ii} of semiconduct-

ing nanotubes as they vary the temperature of the frozen D_2O. Because of the nanotubes' large aspect ratio the resulting compression and expansion is along the axial direction. In the case of uniaxial expansion Eq. (1) fits their data extremely well, proving that the thermal expansion of the host can exert a highly nonisotropic stress on the nanotubes.

It is tempting to attribute the downshifts observed in Table I to isotropic thermal expansion of the nanotubes, which predicts a universal downshift of E_{ii} with increasing temperature. However, it would require a thermal expansion coefficient of $2 \times 10^{-5}/°\mathrm{C}$ to explain our largest thermal shift of -50 meV in the $-160\,°\mathrm{C}$ to $300\,°\mathrm{C}$ temperature range. This is more than 1 order of magnitude larger and opposite in sign from that of graphite ($-1 \times 10^{-6}/°\mathrm{C}$) [25]. Molecular dynamics simulations have predicted the thermal expansion of nanotubes to be similar to that of graphite [26,27]. We therefore favor e-p coupling as the true physical phenomenon underlying the experimental observations. The e-p coupling model is further corroborated by ensemble measurements of the bandgap photoluminescence of nanotubes suspended in air, which show downshifts of E_{11} on the order of 20 μV/K [7], well within the range predicted by the e-p coupling model [15].

In conclusion, tunable Raman spectroscopy is used to measure small changes in the optical transition energies E_{ii} of individual carbon nanotubes over a wide temperature range. For nanotubes suspended over trenches we observe a decrease in E_{ii} with temperature, in contrast to previous measurements on bundles and surfactant coated nanotubes. Theoretical modeling suggests that the temperature dependence of the optical transition energies E_{ii} of nanotubes suspended in air is dominated by the effect of electron-phonon coupling, whereas that of nanotubes coated in surfactant and nanotubes in bundles is dominated by the thermal expansion of the nanotubes' environment.

The authors would like to thank Tim McClure and Mildred Dresselhaus for helpful discussions. This research was supported in part by NSF Grants No. DMR-04-05538, No. DMR04-39768, No. DMR-02-44441, No. NIRT ECS-0210752, No. NSEC PHY-01-17795, U.S. Department of Energy under Contract No. DE-AC03-76SF00098, and Boston University SPRInG grant. Computational resources were provided by NPACI and NERSC. This work made use of MRSEC shared facilities supported by the National Science Foundation under Grant No. DMR-0213283.

*Email address: scronin@usc.edu
Electronic address: http://www-rcf.usc.edu/~scronin/

[1] S. J. Tans, A. R. M. Verschueren, and C. Dekker, Nature (London) **393**, 49 (1998).
[2] J. A. Misewich, R. Martel, Ph. Avouris, J. C. Tsang, S. Heinze, and J. Tersoff, Science **300**, 783 (2003).
[3] H. D. Li, K. T. Yue, Z. L. Zhan, L. X. Zhou, S. L. Zhang, Z. J. Shi, Z. N. Gu, B. B. Liu, R. S. Yang, H. B. Yang, G. T. Zou, Y. Zhang, and S. Iijima, Appl. Phys. Lett. **76**, 2053 (2000).
[4] N. R. Raravikar, P. Keblinski, A. M. Rao, M. S. Dresselhaus, L. S. Schadler, and P. M. Ajayan, Phys. Rev. B **66**, 235424 (2002).
[5] Although the optical excited states are strongly bound excitons (see Ref. [6]), we use the standard E_{ij} notation here to indicate that these excitations are excitons composed of transitions predominately from the ith occupied to the jth unoccupied subbands. In this Letter we focus on the second transition in semiconducting nanotubes, E_{22}^S, and the first transition in metallic nanotubes, E_{11}^M.
[6] C. D. Spataru, S. Ismail-Beigi, L. X. Benedict, and S. G. Louie, Phys. Rev. Lett. **92**, 077402 (2004).
[7] J. Lefebvre, P. Finnie, and Y. Homma, Phys. Rev. B **70**, 045419 (2004).
[8] H. Htoon, M. J. O'Connell, P. J. Cox, S. K. Doorn, and V. I. Klimov, Phys. Rev. Lett. **93**, 027401 (2004).
[9] S. M. Bachilo and R. B. Weisman, *Abstracts of papers of the American Chemical Society, Anaheim, CA, 2004* (American Chemical Society, Washington, DC, 2004).
[10] L.-J. Li, R. J. Nicholas, R. S. Deacon, and P. A. Shields, Phys. Rev. Lett. **93**, 156104 (2004).
[11] K. Arnold, S. Lebedkin, O. Kiowski, F. Henrich, and M. M. Kappes, Nano Lett. **4**, 2349 (2004).
[12] R. M. Martin and L. M. Falicov, *Light Scattering in Solids I*, edited by M. Cardona, Topics in Applied Physics Vol. 8 (Springer Verlag, Berlin), pp. 79–95.
[13] C. Fantini, A. Jorio, M. Souza, M. S. Strano, M. S. Dresselhaus, and M. A. Pimenta, Phys. Rev. Lett. **93**, 147406 (2004).
[14] H. Telg, J. Maultzsch, S. Reich, F. Hennrich, and C. Thomsen, Phys. Rev. Lett. **93**, 177401 (2004).
[15] R. B. Capaz, C. D. Spataru, P. Tangney, M. L. Cohen, and S. G. Louie, Phys. Rev. Lett. **94**, 036801 (2005).
[16] Y. Yin, S. B. Cronin, A. Walsh, A. Stolyarov, M. Tinkham, A. Vamivakas, W. Bacsa, S. Ünlü, B. Goldberg, and A. Swan, cond-mat/0505004 (to be published).
[17] M. S. Strano, J. Am. Chem. Soc. **125**, 16 148 (2003).
[18] F. Wang, G. Dukovic, L. E. Brus, and T. F. Heinz, Science **308**, 838 (2005).
[19] C. L. Kane and E. J. Mele, Phys. Rev. Lett. **93**, 197402 (2004).
[20] L. Yang, M. P. Anantram, J. Han, and J. P. Lu, Phys. Rev. B **60**, 13 874 (1999).
[21] S. B. Cronin, A. K. Swan, M. S. Ünlü, B. B. Goldberg, M. S. Dresselhaus, and M. Tinkham, Phys. Rev. B **72**, 035425 (2005).
[22] Y. N. Gartstein, A. A. Zakhidov, and R. H. Baughman, Phys. Rev. B **68**, 115415 (2003).
[23] R. B. Capaz, C. D. Spataru, P. Tangney, M. L. Cohen, and S. G. Louie, Phys. Status Solidi (b) **241**, 3352 (2004).
[24] M. J. O'Connell, S. M. Bachilo, C. B. Huffman, V. C. Moore, M. S. Strano, E. H. Haroz, K. L. Rialon, P. J. Boul, W. H. Noon, C. Kittrell, J. Ma, R. H. Hauge, R. B. Weisman, and R. E. Smalley, Science **297**, 593 (2002).
[25] W. C. Morgan, Carbon **10**, 73 (1972).
[26] P. K. Schelling and P. Keblinski, Phys. Rev. B **68**, 035425 (2003).
[27] H. Jiang, B. Liu, Y. Huang, and K. C. Hwang, J. Eng. Mater. Technol. **126**, 265 (2004).